



Short communication

## Evaluation of positron emission tomography as a method to visualize subsurface microbial processes

Karen Kinsella<sup>a,b</sup>, David J. Schlyer<sup>a,\*</sup>, Joanna S. Fowler<sup>a</sup>, Robert J. Martinez<sup>b</sup>, Patricia A. Sobecky<sup>b</sup>

<sup>a</sup> Brookhaven National Laboratory, Upton, NY 11973, USA

<sup>b</sup> University of Alabama, Tuscaloosa, AL 35487, USA

### ARTICLE INFO

#### Article history:

Received 15 June 2011

Received in revised form 10 January 2012

Accepted 10 January 2012

Available online 18 January 2012

#### Keywords:

Bioremediation

Positron emission tomography

*Rahnella* sp. Y9602

Subsurface

### ABSTRACT

Positron emission tomography (PET) provides spatiotemporal monitoring in a nondestructive manner and has higher sensitivity and resolution relative to other tomographic methods. Therefore, this technology was evaluated for its application to monitor *in situ* subsurface bacterial activity. To date, however, it has not been used to monitor or image soil microbial processes. In this study, PET imaging was applied as a “proof-of-principle” method to assess the feasibility of visualizing a radiotracer labeled subsurface bacterial strain (*Rahnella* sp. Y9602), previously isolated from uranium contaminated soils and shown to promote uranium phosphate precipitation. Soil columns packed with acid-purified simulated mineral soils were seeded with 2-deoxy-2-<sup>18</sup>F]fluoro-D-glucose (<sup>18</sup>FDG) labeled *Rahnella* sp. Y9602. The applicability of [<sup>18</sup>F]fluoride ion as a tracer for measuring hydraulic conductivity and <sup>18</sup>FDG as a tracer to identify subsurface metabolically active bacteria was successful in our soil column studies. Our findings indicate that positron-emitting isotopes can be utilized for studies aimed at elucidating subsurface microbiology and geochemical processes important in contaminant remediation.

© 2012 Published by Elsevier B.V.

### 1. Introduction

Positron emission tomography (PET) is a medical imaging method widely used for visualizing the metabolism of mammalian cells, particularly brain and cancer cells. Recent studies have employed this technique to better understand geochemical transport in subsurface soils by imaging and modeling soil hydrology [1–4]. To the best of our knowledge, PET has not been used to monitor *in situ* subsurface soil prokaryotic communities (as defined by incorporation of radiolabeled tracers). Specifically, this imaging approach could elucidate fundamental biogeochemical processes involved in the bioremediation of metal- and radionuclide contaminated soils such as those present within several U.S. Department of Energy (DOE) legacy sites.

Decades of cold war nuclear weapons research at the DOE Oak Ridge Reservation has resulted in a subsurface groundwater plume that extends over 4 km. Contaminants including uranium, technetium-99, thorium, toxic metals, nitrate, and

volatile organic compounds have been reported at the site (<http://public.ornl.gov/orifc/>). The use of naturally occurring microbial communities for remediation of contaminated subsurface environments has been shown to be a promising approach for uranium (U) sequestration through reductive precipitation or biomineralization [5–9]. Aerobic and facultative bacterial strains such as *Rahnella* sp. Y9602 that are characterized by constitutive phosphatase activity, isolated from the contaminated ORFRC subsurface, have been shown to facilitate U sequestration by promoting uranium phosphate mineralization [5,9–11]. However, subsurface bioremediation of U and other contaminants currently require destructive sampling methods to assess microbial processes. PET imaging could provide an innovative, non-destructive approach for site monitoring and long-term stewardship of contaminated environments.

In this study, PET imaging was employed to visualize *in situ* metabolic activity of a subsurface bacterial strain (*Rahnella* sp. Y9602) that has been shown to promote uranium sequestration in groundwater and soils [5,9,10]. *Rahnella* sp. Y9602 was labeled with 2-deoxy-2-<sup>18</sup>F]fluoro-D-glucose (<sup>18</sup>FDG), a glucose analog commonly used in PET-based imaging of mammalian cells, and incubated in soil columns as a method to track *in situ* microbial processes contributing to changes in subsurface geochemistry. Radiotracers such as a glucose analog commonly used in PET-based imaging of mammalian cells. Our preliminary studies using the glucose analog <sup>18</sup>FDG, suggest that *Rahnella* sp. Y9602 can be tracked

**Abbreviations:** CFU, colony-forming units; <sup>18</sup>FDG, 2-deoxy-2-<sup>18</sup>F]fluoro-D-glucose; FOV, field of view; NB, nutrient broth; ORFRC, Oak Ridge Field Research Center; PES, polyethersulfone; PET, positron emission tomography; SPE, solid phase extraction.

\* Corresponding author. Tel.: +1 631 344 4587; fax: +1 631 344 7350.

E-mail address: [schlyer@bnl.gov](mailto:schlyer@bnl.gov) (D.J. Schlyer).

within columns that can be designed to simulate contaminated soils systems. Here we discuss the feasibility of using PET imaging to identify *in situ* subsurface microbial populations.

## 2. Experimental

### 2.1. Soil columns

Cylindrical columns 42 mm internal diameter by 73 mm internal length, outside diameter 53 mm, outside length 110 mm, were machined from the fluoropolymer Kynar<sup>R</sup> (polyvinylidene fluoride). Columns were designed to fit the microPET detector array (Section 2.4). Screens, glass wool, and 0.45  $\mu\text{m}$  polyethersulfone filters on the column ends distribute flow and minimize fine particle movement out of the columns. Column volume is 101 mL. Fig. 1 is a schematic of the column design and a photograph of the column in the PET scanner.

Columns were packed with mineral soils (Section 2.2) selected to simulate the subsurface and filled from the bottom inlet using an ultralow flow peristaltic pump (Fisher Scientific, Pittsburg, PA) with 1.6 mm or 0.8 mm ID silicone tubing. Flow rates were 3.6–9.0 mL h<sup>-1</sup>.

### 2.2. Simulated soil

As this study was a proof-of-principle application of PET imaging, simulated (artificial) soils were used. Model simulated soils were composed of sized, acid-purified silicon dioxide (Sigma-Aldrich, St. Louis, MO). Residual metal content was  $\leq 200 \text{ mg kg}^{-1}$  calcium and iron, and  $\leq 50 \text{ mg kg}^{-1}$  cadmium, cobalt, copper, nickel, lead, and zinc. Two texture classes were used: fine sand, 150–400  $\mu\text{m}$ , and a simulated silt loam mix of 31% sand, 50% silt, and 19% clay, simulating the B horizons of ORFRC Areas 2 and 3, the vadose zone of uranium-contaminated ORFRC soils [12].

### 2.3. Radiotracers

Two radiotracers labeled with the short-lived positron emitter fluorine-18 (half-life 110 min; endpoint energy 634 keV) were used in this study. [<sup>18</sup>F]fluoride ion was produced on the medical cyclotron at Brookhaven National Laboratory, Upton, NY from the irradiation of oxygen-18 enriched water (H<sub>2</sub><sup>18</sup>O) via the <sup>18</sup>O(p,n)<sup>18</sup>F reaction. Metal residues were removed using a silica-based hydrophilic strong anion-exchanger (Sep-Pak<sup>R</sup> QMA, Waters Corp., Milford, MA). <sup>18</sup>FDG was purchased from Cardinal Health Nuclear Pharmacy, Plainview, NY.

### 2.4. PET instrument and software

PET imaging was carried out using a Siemens microPET R4 scanner (Siemens Medical Solutions, Malvern, PA). PET data were acquired in list-mode format and processed off-line. PET images were visualized using acquisition sinogram and image processing (ASIPro) VM microPET analysis software. (Concorde Microsystems, Knoxville, TN). The microPET instrument has an 8 cm axial field of view and <2 mm spatial resolution.

### 2.5. Imaging column flow

2.0 MBq mL<sup>-1</sup> of [<sup>18</sup>F]fluoride (54  $\mu\text{Ci mL}^{-1}$ ) in 190 ppm potassium [<sup>19</sup>F]fluoride (K<sup>19</sup>F) was pumped into columns filled with fine sand saturated with 10 ppm K<sup>19</sup>F. The 190 ppm K<sup>19</sup>F was used as a carrier for the [<sup>18</sup>F]fluoride. Breakthrough was monitored at the column outlet using a fluoride ion-selective electrode (Orion Fluoride Solid State Combination Electrode, Fisher Scientific, Pittsburg,

PA) with a 12-bit data logger (OM-EL-2-12BIT, Omega Engineering, Stamford, CT).

### 2.6. Radiotracer sorbents

Radiotracer sorbents were utilized to visualize the resolution limits for bacterial colonies in the model soil columns. To identify a radiotracer sorbent material that could act as a surrogate for <sup>18</sup>F-labeled bacterial populations, solid phase extraction (SPE) was used to screen potential <sup>18</sup>FDG sorbents. SPE columns (1.5 mL) were packed with 1–10 g each of a variety of sorbent materials, including silica gel, native silica, functionalized silicas, alumina, and several size fractions of activated carbon. After conditioning the SPE columns with deionized (DI) water, 0.3 MBq mL<sup>-1</sup> (8  $\mu\text{Ci mL}^{-1}$ ) of <sup>18</sup>FDG in 1 mL DI water was applied to the columns, and eluted with three (1 mL) volumes of DI water. <sup>18</sup>FDG retention was measured in a Picker well counter. An activated carbon size fraction between 74 and 285  $\mu\text{m}$  retained  $45 \pm 5\%$  of the radiotracer.

Columns filled with fine sand were randomly seeded with 0.5 mm radius volumes of the 74–285  $\mu\text{m}$  activated carbon sorbent. *Rahnella* sp. Y9602 colonies are approximately 1 mm in diameter. <sup>18</sup>FDG (1.0 MBq mL<sup>-1</sup> (27  $\mu\text{Ci mL}^{-1}$ )) in DI water was pumped into the columns at 9 mL h<sup>-1</sup> for 1 h, followed by DI water at 9 mL h<sup>-1</sup> for 6 h. PET images were collected for 7 h, and reconstructed in 10 min frames.

### 2.7. Bacteria

*Rahnella* sp. Y9602, previously isolated from the ORFRC Area 2 vadose zone, was utilized for these studies. Previous *in vitro* work has shown that this bacterial strain is tolerant to 200  $\mu\text{M}$  of U(VI) and capable of precipitating up to 95% of uranium as chernikovite [H<sub>2</sub>(UO<sub>2</sub>)<sub>2</sub>(PO<sub>4</sub>)<sub>2</sub>] in simulated groundwater containing uranyl acetate [5,9,10].

Soil columns were filled with autoclaved simulated mineral soils and saturated with sterile saline (0.85%, w/v) prior to filling with mid-log phase *Rahnella* sp. Y9602 at a cell density of 10<sup>8</sup> CFU mL<sup>-1</sup> (colony-forming units mL<sup>-1</sup>) in nutrient broth [(NB); 3 g beef extract, 5 g peptone L<sup>-1</sup>]. The mineral soils were autoclaved as a precaution to ensure that only *Rahnella* cells were present when the <sup>18</sup>FDG solution was added. Columns were incubated at ambient temperature (22–25 °C) for 24 h. One hour prior to radiolabeling, 6–9 mL h<sup>-1</sup> of 70% NB was pumped into the columns for 1 h, followed by 60–115 MBq mL<sup>-1</sup> (1.6–3.1 mCi mL<sup>-1</sup>) <sup>18</sup>FDG in 70% NB for 1 h at the same flow rate. A control containing heat-killed cells was prepared by exposing mid-log phase *Rahnella* sp. Y9602 (cell density 10<sup>8</sup> CFU mL<sup>-1</sup>) to 85 °C for 30 min prior to re-suspension in fresh NB.

## 3. Results and discussion

In this proof-of-principle study, we demonstrated the feasibility of using PET to image a soil bacterial strain that has direct relevance for bioremediation activities in metal- and radionuclide-contaminated subsurface environments. To validate that applicability of PET imaging and <sup>18</sup>FDG-labeling for subsurface systems, we conducted a series of experiments to (i) image soil column flow with the [<sup>18</sup>F]fluoride ion as a radiotracer; (ii) determine the image resolution for a radiolabeled microbial population using bacterial colony-sized volumes of radiotracer sorbent, and (iii) examine the possibility of using a radiolabeled glucose analog (<sup>18</sup>FDG) to image the area of a metabolically active bacterial population in a model soil column setup.

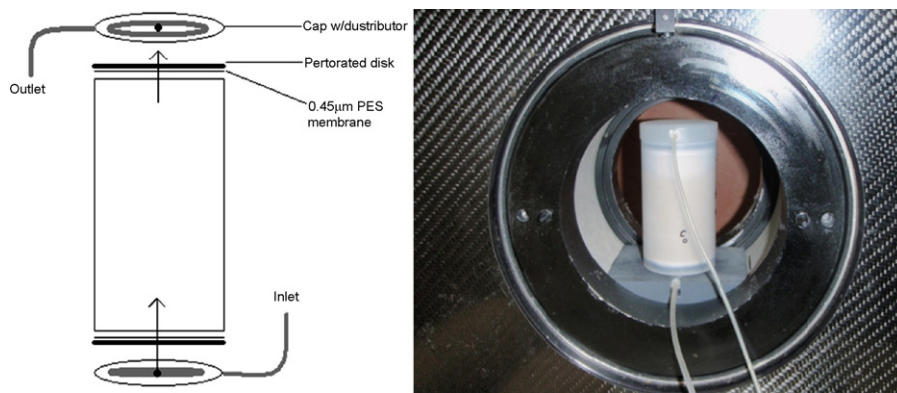


Fig. 1. (Left) Schematic of soil column. (Right) Soil column in microPET scanner.

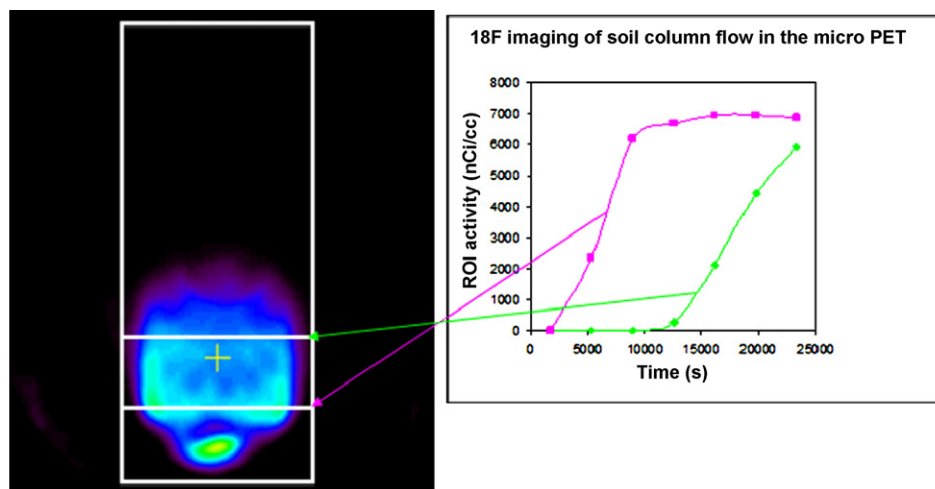


Fig. 2.  $^{18}\text{F}$  microPET image of soil column, as a transverse slice through the center of the column, showing plots of activity ( $\text{nCi cm}^{-3}$ ) vs. time (s) for two regions of interest.  $7000 \text{ nCi} \sim 0.26 \text{ MBq}$ . ROI activity denotes region of interest activity.

### 3.1. Imaging soil column flow

Fig. 2 is a two-dimensional transverse slice through the center of a fine sand column as it is filling with  $2.0 \text{ MBq mL}^{-1}$  ( $54 \mu\text{Ci mL}^{-1}$ ) [ $^{18}\text{F}$ ]fluoride tracer in  $\text{K}^{19}\text{F}$  carrier. Tracer breakthrough monitored by the fluoride ion-selective electrode was equivalent to image timing of the column filled with [ $^{18}\text{F}$ ]fluoride, when corrected for the outlet tube volume. Thus, we posit that the PET images of the soil column demonstrated flow imaging feasibility in this model system.

### 3.2. Imaging radiotracer sorbent surrogate bacterial colonies

In Fig. 3, a two-dimensional PET projection through randomly distributed, bacterial colony-sized volumes of activated carbon in a fine sand column labeled with  $1.0 \text{ MBq mL}^{-1}$  ( $27 \mu\text{Ci mL}^{-1}$ )  $^{18}\text{F}$ FDG is shown. The purpose of these experiments was to validate the feasibility of imaging radiolabeled colonies (populations) of subsurface bacteria using the activated carbon sorbent as a proxy to estimate the minimum *Rahnella* cell concentrations that would be needed for PET imaging in subsequent studies (see Section 3.3). Online Fig. 3 is an animation of the same column, illustrating radiotracer flow over the 7 h collection period.

### 3.3. Radiolabeling of *Rahnella* sp. Y9602

The detection limit of the BNL Siemens microPET R4 is  $0.2\text{--}0.7 \text{ MBq}$  ( $5\text{--}20 \mu\text{Ci}$ ) for the field of view (FOV), a 2 mm slice of

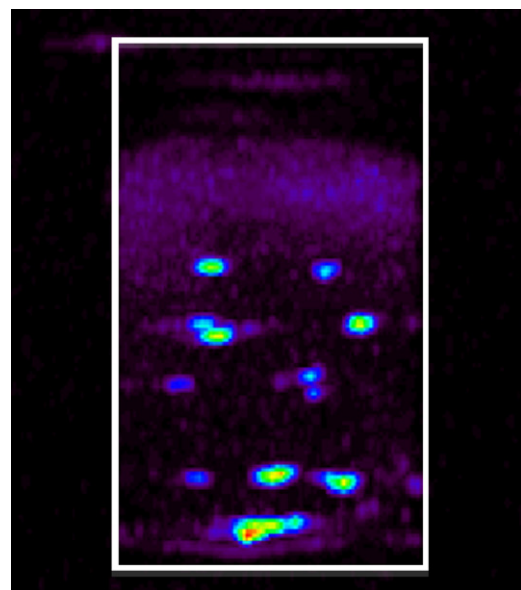


Fig. 3. Two-dimensional PET projection of the soil column filled with fine sand and randomly seeded with activated carbon after exposure to  $1.0 \text{ MBq mL}^{-1}$  of  $^{18}\text{F}$ FDG for 1 h ( $27 \mu\text{Ci mL}^{-1}$ ) followed by 6 h of deionized water, at a flow rate of  $7.2 \text{ mL h}^{-1}$ . Each second represents a 10 min average of 511 KeV annihilation photons.

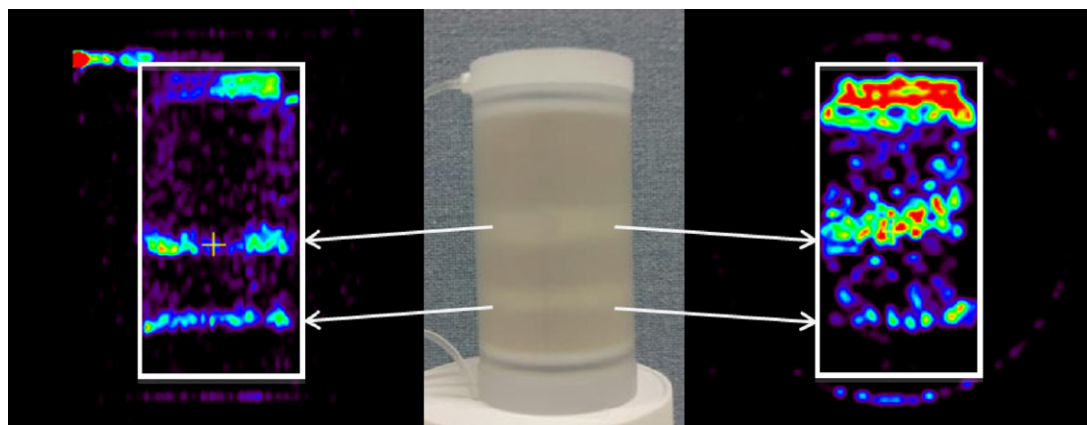


Fig. 4. (Center) Photograph of fine sand column showing two bands of silt loam. (Right and left) PET images of banded column containing  $^{18}\text{F}$ -labeled *Rahnella* sp. Y9602.

the positron source. Considering a 17.5% signal attenuation by silica particles in the soil column, the upper limit of  $0.7\text{ MBq}$  ( $20\ \mu\text{Ci}$ ) is necessary for PET visualization of bacterial colonies (populations). The liquid-filled pore space of our soil column filled with fine quartz sand represents a FOV of approximately  $1\text{ mL}$ . At a cell density of  $10^8\text{ cells mL}^{-1}$  successful PET imaging will require each cell to contain approximately  $7.4\text{ mBq}$  ( $200\text{ fCi}$ ) after decay during the cell labeling and column washing periods. In preliminary *in vitro* labeling experiments conducted with *Rahnella* sp. Y9602 incubated with  $^{18}\text{F}$ -FDG, exposing mid-log cells to  $0.04\text{--}0.07\text{ MBq mL}^{-1}$  ( $1\text{--}2\text{ mCi mL}^{-1}$ ) resulted in uptakes between  $1.8$  and  $7.4\text{ mBq}$  per cell ( $50\text{--}200\text{ fCi CFU}^{-1}$ ; data not shown).

Initially, the soil columns were packed with the simulated silt loam mix in the same texture class as the uranium-contaminated ORFRC subsoil. However, we could not achieve uniform flow through the dense silt loam at flow rates fast enough to accommodate the short half-life of  $^{18}\text{F}$  ( $110\text{ min}$ ) during column imaging ( $7\text{--}9\text{ mL h}^{-1}$ ). In order to visualize bacteria within 6–8 half-lives of the radiotracer addition, the columns were filled with fine sand containing 6 randomly placed  $0.5\text{--}2.5\text{ mm}$  radius volumes of silt loam. PET images of these silt loam-seeded fine sand columns indicated that the majority of the bacteria were flowing out of the column or aggregating on the outlet membrane. An alternative column packing that enabled proof-of-principle method imaging is illustrated in Fig. 4. The center photograph of the soil column shows bands of silt loam,  $10\text{ mm}$  (upper) and  $6.5\text{ mm}$  (lower) thick in a column loaded with fine sand. The images suggest some bacterial colonization of or retention by the silt loam bands. After exposing cells to  $60\text{--}115\text{ MBq mL}^{-1}$  ( $1.6\text{--}3.1\text{ mCi mL}^{-1}$ ) for  $1\text{ h}$  during mid-log phase, then washing with 3 column volumes of unlabeled nutrient medium, the activity in the center of the thicker silt loam band was  $75\text{ kBq cm}^{-3}$  ( $2\ \mu\text{Ci cm}^{-3}$ ). Abiotic and heat-killed cell controls given the same treatment yielded only  $5$  and  $15\text{ kBq cm}^{-3}$  ( $0.13$  and  $0.40\ \mu\text{Ci cm}^{-3}$ ) respectively,  $7$  and  $20\%$  of the live cell activity (data not shown).

#### 4. Conclusions

PET is a nuclear medicine technique that produces three-dimensional images of metabolically active cells and is widely used in clinical diagnostics. Although PET imaging has recently been used for transport monitoring in geomaterials [3], there have no studies to date that employ PET to image and monitor the distribution and presence of subsurface bacteria. In this proof-of-principle study,

our data demonstrate that  $^{18}\text{F}$ -FDG can be used to radiolabel actively growing bacterial cells for subsequent imaging by PET scanning in a model soil system. In this short communication we demonstrate that PET is a promising new approach that could be used to monitor microbial communities in subsurface soils. Future studies will apply this new imaging approach to natural soil systems with intact microbial populations to better understand nutrient cycling and uranium biomineralization in subsurface environments.

#### Acknowledgments

This work was supported by the U.S. Department of Energy Office of Biological and Environmental Research under contract DE-AC02-98CH10886 and partially by DE-FG02-04ER63906.

#### References

- [1] M. Gründig, M. Richter, A. Seese, O. Sabri, Tomographic radiotracer studies of the spatial distribution of heterogeneous geochemical transport processes, *Appl. Geochem.* 22 (2007) 2334–2343.
- [2] W.D. Hoff, M.A. Wilson, D.M. Benton, M.R. Hawkesworth, D.J. Parker, P. Fowles, The use of positron emission tomography to monitor unsaturated water flow within porous construction materials, *J. Mater. Sci. Lett.* 15 (1996) 1101–1104.
- [3] J. Kulenkampff, M. Gründig, M. Richter, F. Enzmann, Evaluation of positron-emission-tomography for visualisation of migration processes in geomaterials, *Phys. Chem. Earth* 33 (2008) 937–942.
- [4] M. Richter, M. Gründig, K. Zieger, A. Seese, O. Sabri, Positron emission tomography for modelling of geochemical transport processes in clay, *Radiochim. Acta* 93 (2005) 643–651.
- [5] M.J. Beazley, R.J. Martinez, P.A. Sobecky, S.M. Webb, M. Taillefert, Nonreductive biomineralization of uranium(VI) phosphate via microbial phosphatase activity in anaerobic conditions, *Geomicrobiol. J.* 26 (2009) 431–441.
- [6] A.J. Francis, C.J. Dodge, F.L. Lu, G.P. Halada, C.R. Clayton, XPS and XANES studies of uranium reduction by *Clostridium* sp., *Environ. Sci. Technol.* 28 (1994) 636–639.
- [7] D.R. Lovley, E.J.P. Phillips, Y.A. Gorby, E.R. Landa, Microbial reduction of uranium, *Nature* 350 (1991) 413–416.
- [8] L.E. Macaskie, R.M. Empson, A.K. Cheetham, C.P. Grey, A.J. Skarnulis, Uranium bioaccumulation by a *Citrobacter* sp. as a result of enzymatically mediated growth of polycrystalline  $\text{HUO}_2\text{PO}_4$ , *Science* 257 (1992) 782–784.
- [9] R.J. Martinez, M. Beazley, M. Taillefert, A. Arakaki, J. Skolnick, P.A. Sobecky, Aerobic uranium(VI) bioprecipitation by metal resistant bacteria isolated from radionuclide and metal-contaminated subsurface soils, *Environ. Microbiol.* 9 (2007) 3122–3133.
- [10] M.J. Beazley, R.J. Martinez, P.A. Sobecky, S.M. Webb, M. Taillefert, Uranium biomineralization as a result of bacterial phosphatase activity: insights from bacterial isolates from a contaminated subsurface, *Environ. Sci. Technol.* 41 (2007) 5701–5707.
- [11] E.S. Shelobolina, H. Konishi, H.F. Xu, E.E. Roden, U(VI) sequestration in hydroxyapatite produced by microbial glycerol-3-phosphate metabolism, *Appl. Environ. Microbiol.* 75 (2009) 5773–5778.
- [12] M.O. Barnett, P.M. Jardine, S.C. Brooks, H.M. Selim, Adsorption and transport of uranium(VI) in subsurface media, *Soil Sci. Soc. Am. J.* 64 (2000) 908–917.